High-precision minmax solution of the two-center Dirac equation

Ossama Kullie

Theoretical Physics at Institute of Physics, Department of Mathematics and Natural Science,
Heinrich-Plett Str. 40, 34132 Kassel, Germany*

We present a high-precision solution of Dirac equation by numerically solving the minmax two-center Dirac equation with the finite element method (FEM). The minmax FEM provide a highly accurate benchmark result for systems with light or heavy atomic nuclear charge Z. A result is shown for the molecular ion H_2^+ and the heavy quasi-molecular ion Th_2^{179+}, with estimated fractional uncertainties of $\sim 10^{-23}$ and $\sim 10^{-21}$, respectively. The result of the minmax-FEM high-precision of the solution of the two-center Dirac equation, allows solid control over the required accuracy level and is promising for the application and extension of our method.

I. INTRODUCTION

It is well known in quantum chemistry that the Dirac equation is subjected to numerical difficulties due to the negative continuum of the spectrum. This causes a variational instability, which makes the numerical computations of one-particle bound states of Dirac equations difficult. In fact, the Dirac energy functional, which is unbounded from both sides is subject to serious implications for variational solutions. Variation of the Dirac functional without efficient discretization of the negative continuum are therefore, subject to the well known variational collapse, positronic contamination and the existence of spurious states. From a numerical viewpoint, the variational collapse and the existence of spurious states are serious problems. The minmax formulation of the relativistic one-particle Dirac equation, which is used in the present work, Refs. [1–5], has a fundamental property, namely an efficient projection against the negative (positronic) continuum. This leads to the minmax energy functional, which guarantees that the solution of the Dirac equation is restricted to the electronic subspace and is well defined for the Coulomb potential with point nuclear charge if $Z < Z_{cr} = 1/\alpha < 137.036..$, otherwise Dirac operator $\widehat{H}_D$ is not well defined as a self-adjoint operator [1]. In the minamx formulation of the Dirac equation, a nonlinear dependence on the eigenvalue occurs. It is, however, even for heavy systems sufficiently weak and does not cause a problem in iterative linearized computations of the eigenvalues. Furthermore, in the non-relativistic limit $(c \to \infty)$ the resulting equation goes over directly into the non-relativistic Schrödinger one, as we will see below. The spectrum is in accord with the variational characterization of the eigenvalues of the Dirac operator based on the minimax principle [6, 7], all levels of the computed spectrum approach the exact Dirac eigenvalue from above with the finer approximation of the space (finer subdivisions by increasing the grid size), and no indication of spurious energy was found.

In the present work, we apply the method developed in earlier studies [6, 7] and perform a high-precision numerical solution of the Dirac equation for an electron in the field of two static positive charges. We achieved an accuracy of $\sim 10^{-28}$ atomic units (au) for H_2^+ increasing the accuracy achieved in the previous work [8] by many orders, and of 10^{-18} au for Th_2^{179+}, which is much better than our earlier result of [7] by many orders as well. The obtained fractional uncertainty of the relativistic $shift$ is $\sim 10^{-23}$, $\sim 10^{-21}$ for H_2^+ and Th_2^{179+}, respectively. The result compares very well with high-precision results recently published in the literature, see below.

The remainder of this paper is organized as follows. In Sec. II, we present a brief introduction to the minimax approach and explain the iteration procedure and non-relativistic limit, the implementation of which is given in Sec. II A. To better follow the results and discussion, we briefly introduce in Appendix A, some of the theoretical basis contained in previous works, in particular references [6–8]. In Sec. III we present our result and discuss the convergence and the accuracy of the FEM calculations. Finally, a comparison with various results from the literature and a conclusion and outlook are presented.

II. METHOD

A solution of the one-particle Dirac equation, a 4-component-spinor ψ, can be obtained from a stationarity principle of the functional $I = \langle\psi|\widehat{H}_D|\psi\rangle - \varepsilon\langle\psi|\psi\rangle$, where $\widehat{H}_D, \varepsilon$ are the one-particle Dirac operator and energy, respectively. However, one cannot apply a variational minimum principle as for the Schrödinger equation, since the spectrum of $\widehat{H}_D$ consists of positive (electronic) and negative (positronic) energies. The main idea of the minmax method, see [1, 5] (and references in [1]), is to consider the the subspace of electronic states (F_+) by projecting out the the subspace of positronic states (F_-) in a two-step search of extrema, where the sequence of minmax level energies is given [1] by

$$\lambda_k = \inf_{\substack{\dim G = k \\ G \text{ subspace of } F_+}} \sup_{\substack{\psi \in (G \oplus F_-) \\ \psi \neq 0}} \frac{\langle\psi \mid \widehat{H}_D \mid \psi\rangle}{\langle\psi \mid \psi\rangle} \, , \tag{1}$$

where $F_+ \oplus F_-$ is an orthogonal decomposition of a well-chosen space of smooth square integrable functions and $I = \langle\psi \mid \widehat{H}_D \mid \psi\rangle/\langle\psi \mid \psi\rangle$ is the energy functional or the Rayleigh quotient, where ψ should not be vanishes (hence the vacuum state $\psi = 0$ is excluded). $\psi = (\psi_1, \psi_2, \psi_3, \psi_4) \equiv (\phi_+, \phi_-)$ is the 4-component relativistic wave function (or short 4-spinor), with the two spinors $\phi_+ = (\psi_1, \psi_2)$ and $\phi_- = (\psi_3, \psi_4)$ which are usually called upper and lower components of ψ and are usually referred to as the large and small component of the 4-spinor ψ. For now, we ignore the dependence on the coordinates, which becomes clear below. As already mentioned the minmax functional in eq. 1 well defined for point nuclear Coulomb potential if $Z < 1/\alpha < 137.036..$), otherwise $\widehat{H}_D$ is not well defined as a self-adjoint operator (for details on this we kindly refer to the review [9]), and it has been proven [1] that the sequence of minmax energies λ_k corresponds to the sequence of positive eigenvalues, which represents the electronic part of the total interval $(-mc^2, +mc^2)$ of $\widehat{H}_D$. In other words, it guarantees the solution of the Dirac equation in the space of the large component ϕ_+, compare eq. 4 below. It is free from spurious states and contaminations that is known

from the 4-spinor calculations. The one-particle Dirac eigenvalue equation of the electron in a scalar potential V, $\widehat{H}_D \psi = \varepsilon \psi$, can be written in the form

$$\begin{pmatrix} V & \widehat{L} \\ \widehat{L} & V - 2m_e c^2 \end{pmatrix} \begin{pmatrix} \phi_+ \\ \phi_- \end{pmatrix} = \varepsilon \begin{pmatrix} \phi_+ \\ \phi_- \end{pmatrix}, \tag{2}$$

where $\widehat{L} = -i\,c\,\hbar\,\boldsymbol{\sigma} \cdot \boldsymbol{\nabla} = -i\,c\,\hbar \sum_{k=1}^{3} \sigma_k \partial/\partial x_k$, where x_k are the space coordinates and σ_k are the Pauli matrices. And because L is a hermitian operator $\langle \phi | L^\dagger = L | \phi \rangle$, we ignore the $\dagger$ sign. By eliminating the small component ϕ_- from eq. (2) one obtains

$$\widehat{L} \left(\frac{\widehat{L} \phi_+}{\varepsilon + 2mc^2 - V} \right) = (\varepsilon - V)\, \phi_+ \ , \tag{3}$$

ε is the eigenenergy that in the non-relativistic limit corresponds to the eigenenergy of the Schrödinger equation. Eq. (3) can be now transformed into the minmax integral "weak" form, which offers a good efficiency for FEM with large finite-element basis set, leading to the equation,

$$\int \frac{c^{-2}|L\phi_+|^2}{2m_e + (\varepsilon - V)/c^2} dr^3 = \int (\varepsilon - V)\, |\phi_+|^2 dr^3 \ . \tag{4}$$

The minmax principle now guarantees the minimum of the energy value ε as mentioned above [1]. Obviously, the two equations (3), (4) bear similarities to their non-relativistic counterparts, the Schrödinger equation and its integral "weak" form since $\lim_{c \to \infty} (\varepsilon - V)/c^2 = 0$, in which the two components ψ_1, ψ_2 of the ϕ_+ transform into their non-relativistic counterparts $\phi_\uparrow, \phi_\downarrow$ (they are degenerate in the absence of a magnetic field interaction). However, eqs. (3), (4) are nonlinear in the eigenvalue ε and therefore have to be solved by iteration. The nonlinearity is weak hence the left-hand side of eq. (4) is expanded in a series [1] as follows. With an approximate value ε_0 of an eigenvalue ε, the iteration procedure at iteration $j+1$ ($j = 0, ..., j_{\max}$) consists of expanding the left-hand side as [6],

$$\int \frac{|L\phi_+|^2}{\varepsilon^j + 2m_e c^2 - V} dr^3 = \int \frac{|L\phi_+|^2}{g(\varepsilon_0)} dr^3 + \sum_{k=1}^{k_{\max}} (-\Delta \varepsilon^j)^k \int \frac{|L\phi_+|^2}{g(\varepsilon_0)^{k+1}} dr^3 \ , \tag{5}$$

with $g(\varepsilon_0) = \varepsilon_0 + 2m_e c^2 - V$ and $\Delta \varepsilon^j = \varepsilon^j - \varepsilon_0$. The first term, the matrix elements, on the right-hand side of eq. 5 is computed once and stored for the next iterations. The second term is updated on each iteration $j \geq 1$, requiring only multiplication operations and a sum over k. The series converges rapidly, where $k_{\max} = 3 - 9$ is sufficient for $Z = 1 - 90$ since is it easy to guess an approximate value ε_0 (e.g. from non-relativistic values). The matrix equation is solved by an iterative method with a Cholesky decomposition [10], which is the heaviest part of the computation. More details can be found in [6, 10].

In our FEM approach, as we will see in the next section, we perform the computation for a series of successive grids and the approximate solution of one grid is used to start the next finer grid. Compared to the 4-spinor formulation, the minmax formulation exhibits major advantages: only 1/3 of the matrix elements of the 4-spinor formulation, have to be computed and the vector iteration requires a factor 4 less operations [6, 7]. The reduced size of the problem enhances the computational performance considerably, as we will see in the present work.

We have seen that in the limit $(c \to \infty)$, eq. (4) transforms directly to the non-relativistic the integral "weak" form of the Schrödinger equation and therefore is expected to exhibit similar properties to the non-relativistic case. The non-relativistic eigenvalue is calculated by setting c to a large number (in the present work $c > 10^{+15}$, $\alpha^2 < 10^{-30}$, the uncertainty is of the order $(\delta \alpha)^2 \sim 10^{-31}$, see further below). This has an important advantage that the the relativistic *shift* is extracted with a better accuracy than the directly calculated values, due to error cancellation (see Sec. III). It is known in computational chemistry by the acronym counterpoise.

A. Solution of the two-center Dirac equation with FEM

The Dirac Hamiltonian in au for a single-particle (of mass $m = 1$) in a two-center potential V is

$$H_D = c\,\boldsymbol{\alpha} \cdot \mathbf{p} + c^2 \beta + V \ , \tag{6}$$

$$V = -\sum_{l=1}^{2} \frac{Z_l}{|\mathbf{r} - \mathbf{R}_l|} \ .$$

N_e/N	Relativistic, E_{rel}	Non-relativistic, E_{nrel}	Rel. *shift* ΔE_{rel} (10^{-6})
72/3721	**-1.10264158**076265658336304	**-1.1026342122500083644351**	**-7.3665376**55746919537216
128/6561	**-1.10264158103**129731540804	**-1.1026342149**366618700516	**-7.3665376311**28402879085
200/10201	**-1.10264158103254**876503352	**-1.1026342149491**805349370	**-7.36653763071**1539825949
288/14641	**-1.10264158103257**440524021	**-1.1026342149494**370230232	**-7.366537630702**937883947
392/19881	**-1.10264158103257701**626914	**-1.1026342149494**631361918	**-7.3665376307026**49958534
512/25921	**-1.10264158103257716**018477	**-1.1026342149494645**757546	**-7.3665376307026093**05534
648/32761	**-1.10264158103257716288**008	**-1.1026342149494646**027071	**-7.3665376307026093**65171
800/40401	**-1.10264158103257716398**460	**-1.1026342149494646137**541	**-7.366537630702609**181867
968/48841	**-1.10264158103257716409**888	**-1.1026342149494646148**972	**-7.36653763070260915**7530
1152/58081	**-1.10264158103257716411**642	**-1.1026342149494646150**726	**-7.36653763070260915**6421
1352/68121	**-1.10264158103257716411**686	**-1.1026342149494646150**770	**-7.36653763070260915**6250
1568/78961	**-1.10264158103257716411**800	**-1.1026342149494646150**884	**-7.366537630702609156**039
1800/90601	**-1.10264158103257716411**811	**-1.1026342149494646150**895	**-7.366537630702609156**055
extp[1]	**-1.10264158103257716411814**	**-1.1026342149494646150898**	**-7.3665376307026091560584**

TABLE I: Energies of H_2^+ at $R = 2$. All values in atomic units. The calculations utilize $\nu = 8$ and $D_{\max} = 40$. N_e, N are the numbers of the elements and grid points respectively. Last digit is rounded. Superscript [1] indicates values extrapolated over the sequence N_e. Bold digits are significant.

where $\boldsymbol{\alpha}$ and β the usual Dirac matrices, $\mathbf{p}$ is the momentum. Z_1, Z_2 are the charges of the two nuclei in units of the elementary charge, $\mathbf{r}$ is the position of the electron, and $\mathbf{R}_l$ are the positions of the nuclei. In the two-center case one has axial symmetry around the internuclear axis (the z-axis), which suggests the use of prolate spheroidal (elliptic spheroidal) coordinates ξ, η and φ. A further singular coordinate transformation $(\xi(s), \eta(t))$, see eq. (A1), is required to deal with the Coulomb singularity of point nucleus. It guarantees a high order of convergence that allows full use of the higher FEM (approximation) order p, as it provides an efficient description of the singularity of the wave function in the vicinity of the nuclei [11–13].

Due to axial symmetry the angular dependence is separated analytically by the ansatz:

$$
\psi \;=\; \left(\begin{array}{c} \phi_+(s,t,\varphi) \\ \phi_-(s,t,\varphi) \end{array} \right) = \left(\begin{array}{c} \phi^1(s,t) \cdot e^{i(j_z-1/2)\cdot\varphi} \\ \phi^2(s,t) \cdot e^{i(j_z+1/2)\cdot\varphi} \\ i\phi^3(s,t) \cdot e^{i(j_z-1/2)\cdot\varphi} \\ i\phi^4(s,t) \cdot e^{i(j_z+1/2)\cdot\varphi} \end{array} \right) \quad . \tag{7}
$$

the z-component of the total angular momentum j_z, is a good quantum number and the relativistic wave function ψ is an eigenstate of the total angular momentum and its z-component j_z. With the Hamiltonian H_D of eq. 6, and eqs (2)-(7) the two dimensional Dirac equation is transformed into eigenvalue matrix equation, which is solved numerically by FEM (and iteratively), as already mentioned [8]. The 2-dimensional domain (s,t) is subdivided into FEM triangular elements and the components $\phi^k(s,t)$ are approximated using global functions and a complete polynomials of an order p in s,t [14], see Appendix Sec A2.

III. RESULT AND DISCUSSION

In the present work, we compute the ground state energy $\varepsilon_{1(1/2)g}$, i. e. with $j_z = 1/2$ and gerade symmetry g, for two molecular ions H_2^+ and Th_2^{179+}. The notation of the corresponding non-relativistic state is $1\sigma_g$. We abbreviate the notation by the short-hand E_{rel}, E_{nrel}, respectively. In our calculation, unless otherwise specified, we use atomic units and the CODATA 2018 value of $c = \alpha^{-1} = 137.035999084$ [15].

In the following, the notation p denotes the order of a two-variable, complete polynomial (FEM-approximation), and ν refers to the values generating the sum of the singular coordinate transformation, see eq. A1. Further notations will be explained in the text. In the presented calculations, we use the FEM polynomial order $p = 10$, which approximately guarantees a convergence order ~ 10 in the calculation by suitable ν value of the singular coordinate transformation of eq. A1, as we will see below. We run test calculations for different values of ν and size of the domain in order to check and reach the highest convergence. The size is defined by the size of the largest ellipse $\xi = \xi_{\max} = const.$ containing the grid elements. The size of the grid can alternatively be defined by $D_{\max}(\xi_{\max})$, defined as the distance (perpendicular to the connecting line of the two centers) between one of the centers to a point on the outermost ellipse ξ_{max}[16]. It was found that the optimal $D_{\max}$ values (given in atomic units) of ~ 40 for H_2^+ and ~ 0.35 for Th_2^{179+}. However, as shown below, the precise value of $D_{\max}$ is not crucial. It should be compared to the internuclear distance,

(a) $D_{\max} = 40\,au$, $\nu = 8$, good convergence.

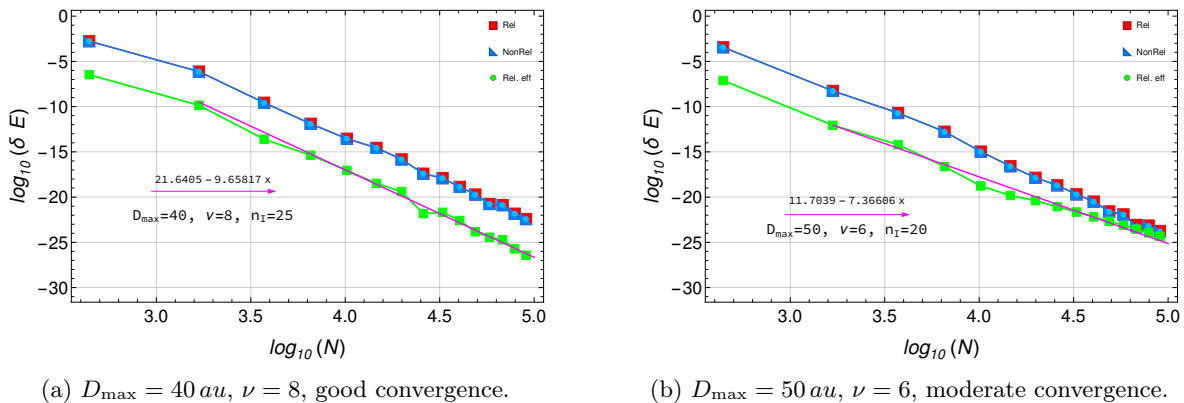(b) $D_{\max} = 50\,au$, $\nu = 6$, moderate convergence.

FIG. 1: (Color online) Convergence behavior of the relativistic (red square) and non-relativistic (blue, left triangle) energies and of the relativistic *shift* (green circle) for H_2^+, as a function of the number of grid points N. $\delta E = |E^{\text{extp}} - E(N)|$ (see table I, where the first two points are omitted). Two cases are shown. (a): $D_{\max} = 40\,au$, $\nu = 8$, highest possible convergence order of polynomial approximation $p = 10$ (see table I). (b): $D_{\max} = 50\,au$, $\nu = 6$, a moderate convergence order, which is considerbly below the FEM order of p=10 (values are not shown).

$R = 2$, $R = 2/90$ for the H_2^+ and Th_2^{179+}, respectively. $R = 2$ is the approximate equilibrium bond length of the H_2^+ molecule, whereas $R = 2/90$ is scaled over the atomic number $Z = 90$ for Th_2^{179+}.

In table I, we show the calculated energies for the ground state of the H_2^+. In the first column the element and point number of the grids are given. The relativistic E_{rel} and non-relativistic E_{nrel} energy values are given in the columns $2, 3$. As seen in the table the accuracy increased systematically for both values of E_{rel} and E_{nrel}. The relativistic *shift* is given in column 4, which is calculated by the simple relation $\Delta E = E_{\text{rel}} - E_{\text{nrel}}$. The absolute uncertainty of the relativistic *shift* is better than the calculated values of the respective energies, benefiting from error compensation [7] by considering the non-relativistic energy E_{nrel} for the same grid and parameters. In addition, table I (last row) shows the extrapolated values [6, 7, 17] over grid elements (or grid points as both sequences scale similar). For clarity, bold digits indicate significant digits. As seen in table I, the accuracy increases with increasing number of grid points (finer subdivision), and that the convergence to the exact (lower energy value) is from above, not only for the non-relativistic but also for the (Dirac) relativistic energy value, which is not surprising (see Sec. II), and is a major advantage of minmax approach, which effectively projects the problem onto the electronic states.

In Fig. 1, we present a log-log plot of the errors $\delta E(N)$ of the energies and of the relativistic *shift*, with respect to the extrapolated value (the last row in table I). As can be seen from the red and blue colored lines (points) in Fig. 1, the convergence rate in the (relativistic) minmax formulation is close to that of the non-relativistic Schrödinger formulation [18]. Concerning the convergence, a high value of ν (e.g. $\nu = 8$) in the coordinate transformation eq A1 is needed (especially for grids with a large number of points, compare Fig. 1), which in turn enables a higher convergence order for the energy and the full utilization of a higher FEM order approximation $p = 10$ [7, 11, 16].

For a larger ν value (Fig. 1a), the wave function is better approximated near the two centers, and the error of the relativistic singularity eq. A4 becomes significantly small also for the dense grids. Here, a suitable distribution of the grid points between the inner and outer regions over the domain is thereby achieved. This optimizes error compensation and achieves better accuracy in the relativistic *shift* (green colored). As an illustration, we performed calculations for the same grids as in table I but with a lower value $\nu = 6$ and present the corresponding log-log plot in Fig. 1b. From the linear fit on the relativistic *shift* shown in the Fig. 1a, using $\nu = 8$, one finds a convergence order $q \approx 9.7$, which is close to the FEM order of $p = 10$, unlike in the Fig. 1b, where $q \approx 7.4$ is considerably smaller than the FEM order $p = 10$, especially an optimal cancellation of the errors is not achieved for larger grids. As seen in Fig. 1, the estimated uncertainties of the computed energies are $\sim 10^{-23}$, and for the relativistic *shift* is $\sim 10^{-28}$ or a fractional uncertainty of $\sim 10^{-23}$ in the relativistic *shift* (see also below table V).

$D_{\max}$	value for densest grid	extrapolated value
30	$-7.3665376307026091560591$	$-\mathbf{7.36653763070260915605}76$
40	$-7.3665376307026091560546$	$-\mathbf{7.36653763070260915605}83$
50	$-7.3665376307026091560635$	$-\mathbf{7.36653763070260915605}81$
60	$-7.3665376307026091560496$	$-\mathbf{7.366537630702609156025}0$

TABLE II: Dependence of the relativistic *shift* ΔE_{rel} (in 10^{-6} atomic units) at $R = 2$ on the domain size $D_{\max}$. The result is for the densest grid with 1800/90601 elements/points. All evaluations were performed with $\nu = 8$. Bold digits are significant
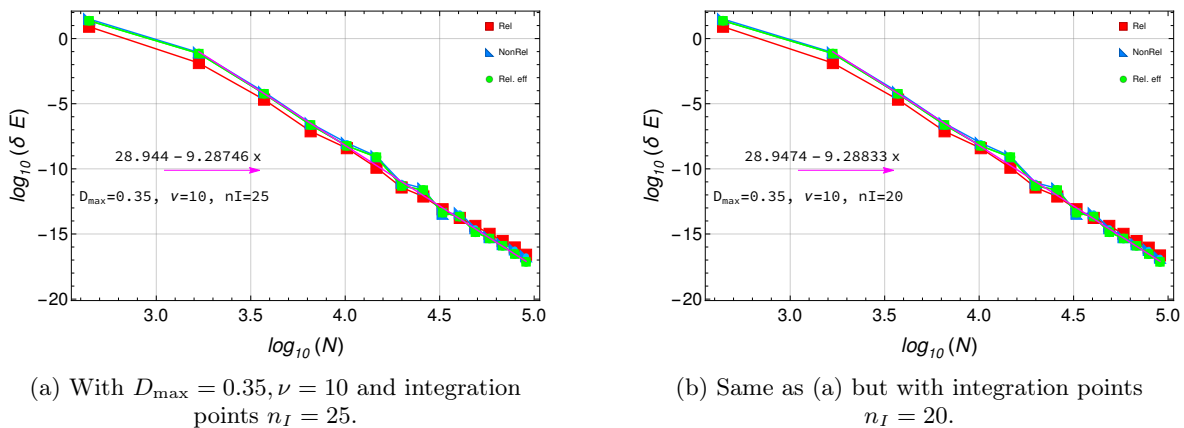
(a) With $D_{\max} = 0.35, \nu = 10$ and integration points $n_I = 25$.

(b) Same as (a) but with integration points $n_I = 20$.

FIG. 2: (Color online) Same as in Fig. 1, for the quasi-molecular ion Th_2^{179+}. (a) and (b) are calculated with $D_{\max} = 0.35, \nu = 10$ and FEM polynomial approximation order $p = 10$. For (a) compare table III (whrer the first two points are omitted).

Table II shows the dependence of the relativistic *shift* on the domain size D_{max} and makes it clear that the exact value of the domain size does not matter. Table II indicates that the optimal value is in region $D_{\max} \sim 40$. In fact, a moderate variation of $D_{\max}$ mainly affects the outer region; therefore, due to the error cancellation, the relativistic *shift* is not sensitive to $D_{\max}$.

N_e/N	Relativistic, E_{rel}	Non-relativistic, E_{nrel}	Rel. *shift* ΔE_{rel}
72/3721	**-9504.75662**77711897646180	**-8931.337**058411524371542	**-573.4195**693596653930759
128/6561	**-9504.7566483**577412426133	**-8931.337137**096470274648	**-573.4195112**612709679648
200/1020	**-9504.7566484**301451994401	**-8931.337137**399365527444	**-573.4195110**307796719956
288/14641	**-9504.756648433**886680448	**-8931.33713740**8143475088	**-573.4195110**257432053607
392/19881	**-9504.756648434**005781759	**-8931.3371374090**57756356	**-573.41951102494**80254030
512/25921	**-9504.7566484340**08746274	**-8931.337137409063**219487	**-573.41951102494**55267868
648/32761	**-9504.7566484340**09421628	**-8931.337137409066**302506	**-573.419511024943**1191218
800/40401	**-9504.756648434009**483622	**-8931.337137409066**299523	**-573.419511024943**1840987
968/48841	**-9504.756648434009**496581	**-8931.3371374090663**35431	**-573.419511024943**1611496
1152/5808	**-9504.756648434009**499723	**-8931.3371374090663**37662	**-573.41951102494316**20606
1352/68121	**-9504.75664843400950**0459	**-8931.3371374090663**38069	**-573.41951102494316**23896
1568/78961	**-9504.75664843400950**0656	**-8931.3371374090663**38170	**-573.41951102494316**24852
1800/90601	**-9504.756648434009500**723	**-8931.3371374090663**38216	**-573.41951102494316**25066
extp^1	**-9504.756648434009500**748	**-8931.337137409066338**235	**-573.419511024943162**514

TABLE III: Energies of Th_2^{179+} at $R = 2/90$. All values in atomic units. The calculations utilize $\nu = 10$ and $D_{\max} = 0.35\,au$. N_e, N are the numbers of the elements and grid points respectively. Last digit is rounded. Superscript [1] and bold digits as in table I.

For systems with high atomic nuclear charge Z, such as our calculated system Th_2^{179+}, it has already been shown [6], [7] that the minmax formulation behaves much better than the 4-spinor formulation. The achieved accuracy of the calculations is significantly higher, while the computational effort is lower. In table III, we report our result for Th_2^{179+} for the same grid sequence used in table I for H_2^+. For Th_2^{179+}, a small domain size $D_{\max} = 0.35\,au$ and $\nu = 10$ are used. Similar to H_2^+, despite the strong singularity, one finds a convergence from above towards the exact values of the non-relativistic and the Dirac relativistic energies, which demonstrates the power of the FEM-minmax method. The absolute accuracy is reduced compared to the H_2^+, this is because for high-Z the singular behavior is much stronger and a higher density of the grid points needed for the regularization of the singularity near the nucleus. This in turn affects the approximation error (dilutes the point density) at large distance from the centers. The value of $\nu = 10$ is large but still the singularity error outweighs the convergence order. This can be seen in Fig. 2, where similar to Fig. 1, we show a log-log plot of the errors $\delta E(N)$ of the energies and the relativistic *shift* relative to the extrapolated value (the last row in table III). As seen in Fig. 2, the error in the relativistic *shift* is only slightly better than in the energy values, unlike what we found in H_2^+, since the singularity error hinders an efficient cancellation of the smooth FEM (or the FEM-approximation) error at the outer region far from the nucleus. Nevertheless, a convergence order $q \approx 9.3$ is reached, it is below the FEM order of 10, although it is not far from that of H_2^+, as seen from the linear fit in Figs. 1, 2.

To test the accuracy and the convergence of the result by checking the accuracy of the matrix element, we achieved

D_{max}	E_{rel}
0.300	-9504.7566484340095007351
0.325	-9504.7566484340095007376
0.335	-9504.7566484340095007368
0.350	-9504.7566484340095007373
0.365	-9504.7566484340095007383
0.375	-9504.7566484340095007387
0.400	-9504.7566484340095007371

TABLE IV: Scatter of the extrapolated values E_{rel} as a function of D_{max} around the value given in Table V. A lower limit of E_{rel} is -9504.75664843400950074, which is slightly shallower than the extrapolated value given in table III.

similar calculations but with smaller integration point per (triangular FEM) element $n_I = 20$ instead of $n_I = 25$ per element. The result is log-log plotted in Fig. 2b, in a similar way to Fig. 2a. The two results with $n_I = 25, n_I = 20$ show a similar behavior. They illustrate and confirm that the (lower) convergence behavior is caused by the singularity near the centers at such a high Z. A similar test is done for H_2^+, it was found that the effect of the integration point between $n_I = 20$ and $n_I = 25$, is of the order $\delta\varepsilon(n_I = 20 \to n_I = 25) \sim 10^{-29}$. And using $n_I > 25$ does not improve the accuracy.

The value of $D_{\max}$ is also not crucial for the calculation or Th_2^{179+}, but the error cancellation ($E_{\mathrm{rel}} - E_{\mathrm{nrel}}$) is more sensitive to $D_{\max}$ than for H_2^+. It turns out that a range around $D_{\max} \sim 0.35$ is optimal, as can be seen in Fig. 2, in which an optimal balance is achieved between short-range error (singularity error) and long-range error, which is on the order of the FEM approximation.

We checked this behavior for different $D_{max} = 0.25 - 0.50$, the result is shown in table IV. A look at the table shows that the unbalanced distribution of the grid points between inner and outer regions causes some oscillatory behavior in the relativistic effect, see also below. From Fig. 2 and table III it can be seen that the uncertainties in the relativistic energy are estimated at $\sim 10^{-18}$, or a fractional uncertainty of 10^{-21} in the relativistic *shift*, which is two orders of magnitude worse than for H_2^+.

Finally, we note that for an effective error cancellation, we use the same ν of the singular coordinate transformation for the non-relativistic calculation, although the smallest value of the singular coordinate transformation $\nu = 2$ for non-relativistic calculations is sufficient. Using $\nu = 2$ does not condense the points in the inner region, which means that the density of the points in the outer region (far from the core) are not diluted, resulting in better accuracy than with a higher ν value for the same grid points in the non-relativistic calculations. By adding the relativistic *shift* to the non-relativistic values calculated with $\nu = 2$, one obtains more accurate relativistic energy value, which is done in table V that shows our final result with a comparison to a recent available result from the literature [19]. However, due to the extrapolation the values for different D_{max} scatter and a limited gain in the accuracy is reached. Table IV shows this behavior and demonstrate the reliability of our final result for Th_2^{179+} in table V.

	H_2^+	Th_2^{179+}
Rel. eff.	-0.0000073665376307026091560584	-573.4195110249431625138
Nrel.	-1.1026342144949464615089689415	-8931.3371374090663382226
Rel.	-1.102641581032577164118124999995	-9504.756648434009500737
[19]	-1.1026415810325771641181249999957656	-9504.756648434009500732

TABLE V: Final result and a comparison with the recent available result from the literature.

Looking at table V on finds an excellent agreement with the result of Nogueira et. al. [19]. The discrepancies are $\sim 7.10^{-30}, 5.10^{-18}$ (where the last digits are rounded) for H_2^+, Th_2^{179+}, respectively. We have to add that the extrapolated value E_{nrel} in table V was obtained with $\nu = 2$ and $D_{max} = 80, 0.80\,au$ for H_2^+ and Th_2^{179+}, respectively, and the (extrapolated) relativistic *shift* was obtained by using the convergence orders, $q = 9.7, 9.3$ as shown in Figs 1, 2, respectively. Where q is the leading order of the polynomial or rational (function) approximation of the error. It changes slightly by changes of the parameters, where in general the discrepancy scatters around $\lesssim 10^{-29}, \lesssim 10^{-18}$ or fractional uncertainties of $\sim 10^{-23}, \sim 10^{-21}$ for H_2^+, Th_2^{179+}, respectively. This sets the limits of accuracy in our result, considering the various parameters and highest grid points used in table I, III. One notices that the extrapolated values of E_{rel}^{extp}, E_{nrel}^{extp} in tables I, III (in the second and third columns) are slightly lower than the value given in table V. That is because the extrapolation of E_{nrel}, E_{rel} usually yields a lower value than the "exact" one, but for the relativistic effect a correction in the opposite direction (counterpoise effect) is achieved. And usually the value $E_{\mathrm{rel\,shift}}^{extp}$ is better than the difference $E_{\mathrm{rel}}^{extp} - E_{\mathrm{nrel}}^{extp}$. While in the first case the extrapolation is performed once, in the second case the extrapolated result of E_{rel}^{extp}, E_{nrel}^{extp} could occur in opposite directions. Considering the comparison to

the work of Nogueira et. al. [19], our FEM minmax methods behaves better in the relativistic domain, because of two aspects. First, the minmax guarantees convergence from above, and second, it is free from spurious states and thus free from contamination (see also Fillion et al. [20]), whereas the authors of [19] have reported such states in the calculations for $Z = 90$. This never has been detected in our FEM calculation so far for $Z = 90$, see ref. [18]. In our calculation, we find $2N$ (N is the grid points number) positive eigenvalues corresponds to the large (2-component) spinor ϕ_+ of the Dirac wave function, see Secs. II, II A. Taking these two aspects into account, we think that our final result in table V for the highly relativistic Th_2^{179+} is slightly better than the values of [19], although for H_2^+ the value of [19] is given with more significant digits than our value.

Reference	H_2^+	Th_2^{179+}
Kullie et al. [8], [7]	-1.10264158103360758005[a]	-9504.7567469606[a]
Mironova et al. 2015 [21]	-1.1026415810330	-9504.756746927[a]
Tupitsyn et al. 2014 [22]	-1.1026415810330[a]	-9504.756746927[a]
Fillion-Gourdeau et al. 2012 [20]	-1.102641580782[b,d]	-9504.698874401[b,d]
Artemyev et al. 2010 [23]	-1.1026409[c]	-9504.752[c]
Ishikawa et al. 2008 [24]	-1.102641581033598[a]	
Parpia and Mohanty 1995 [25]	-1.1026415801[a]	-9504.756696[a]
Rutkowski 1999 [26]		-9504.7567151[a]

TABLE VI: Comparison with values for the literature with different α values, for the ground-state energy of the H_2^+, Th_2^{179+} molecular ions at $R = 2$, $R = 2/90$, respectively. [a],[b], [c] The value are obtained with $\alpha^{-1} = 137.0359895$, 137.035999679, 137.036, respectively. [d] Minmax result of ref. [20].

In table VI we present a comparison with result from the literature. It is obvious that the accuracy in these results is not high, but we must point out that these results are obtained with less computational effort than the present work, moreover, the result of ref. [20] is obtained using minmax method. The results presented in the present work serve as a benchmark for the further development of methods in the relativistic domain. Another issue is the accuracy regarding the precision of α value, where the comparison of our result in table V, VI, shows, as expected, that using $\alpha_{old}^{-1} = 137.0359895$ (accuracy on the order $\sim 10^{-6}$ leads to uncertainty in the energy of the order $\Delta E \sim 10^{-12}$, i.e. it is on the order $(\Delta\alpha)^2$. The uncertainty in the α_{New} (CODATA18) used in the present work is of the order $1.5\,10^{-10}$ (see pml.nist.gov) leading to uncertainty of order 10^{-20} in the obtained energies. For H_2^+, this uncertainty is larger than the precision reached in the calculation (this work), but it is smaller for Th_2^{179+} as can be seen from table IV, V, where the uncertainty of the result for is of order $\sim 10^{-18}$. In addition, the accuracies of the values of Th_2^{179+} given in table VI are blow the precision of $(\Delta\alpha_{old}^{-1})^2 = 10^{-12}$.

Finally, in general, the point-like nucleus approximation is most commonly used, which is justified by the large scale difference between the nuclear radii and the internuclear distance. The effect of finite nuclear size (FNS) for low-Z systems is expected to be small (or beyond interests), while it is significant for high-Z systems [23, 27]. The point-like model is typically used to compare different methods and the accuracies achieved.

In our work the higher order of the singular coordinate transformation eq. A1 largely reduces the singular error as shown in Figs. 1, 2 and we would expect that the FNS effect on the relativistic effect is scaled down. Corrections to the values of the physical quantities induced by the FNS are small, see for example [27–30], but they are relevant for comparing with the experiment. For H_2^+ (and HD^+) there is no particular need to improve the calculation of FNS corrections: The leading order is already known [31, 32] and higher-order corrections are too small to be of interest at the present level of accuracy. The FNS correction is important in the case of high-Z systems, especially when calculating QED corrections [33–35].

For the calculations in the present work, we used quadruple precision. The extension of the arithmetic is not required, rather parallelization of our code, which facilitate the computation and also allows higher grid points to be treated than those used in the tables I, III. Furthermore, multi-electron systems could be easily treated in the framework of Hartree-Fock or density functional theory [17, 36]. Concerning the time of the calculation, it depends much on different parameter and the desired accuracy (and various grid sequences of different orders), which also influenced by the number of iteration in each grids, in particular for grids with large grid points. For an example the calculation in table I take about 173 hours for relativistic calulation and 120 hours for nonrelatvistic calulation, on one core (as already mentioned the code is not parallelized). For the same grid sequence the calculation in table III takes about 2.5 times longer for Th_2^{179+}, which is mainly because more iterations are required in the large grids. However, the last three grids in the grids-sequence take 60% of the time, although the gain in the accuracy is only about two or three orders.

Conclusion and Outlook In this work, we presented highly accurate minmax FEM calculations for the ionic molecule H_2^+ and quasi-molecule Th_2^{179+}. We showed systematically accurate values by investigation of the convergence

behavior of the relativistic and non-relativistic numerical solution of the two-center Coulomb problem. Our result is compared with results available in the literature and shows a good agreement with the recently published result. Applications such as the g-factor (tensor) of bound electrons for H_2^+ by perturbative evaluation of the Zeeman energy [33, 37–40] are currently being investigated, taking into account relevant corrections for comparison with the experimental value.

The high-precision relativistic calculations we achieved enables investigation of other properties such as QED corrections. However, the calculations of radiative QED corrections are demanding and necessitate sums over intermediate states[20]. Artemyev et al [34] have done some calculations on heavy one-electron quasi-molecular ion such as U_2^{183+}, the precision they achieved is not high. The most attractive application is the one-loop self-energy, which is currently the main source of theoretical uncertainty in the hydrogen molecular ions [33, 41]. The calculation of the one-loop self-energy in a weak binding field (i.e. low nuclear charges), suffers from a serious loss of numerical precision because of strong cancellations occurring in the renormalization procedure, hence the need for extremely accurate wave functions and energies [42, 43]. Solving the two-center Dirac equation with FEM-minmax, offers the possibility to improve the precision substantially, especially that the minmax solution is free from spurious states and contamination of the negative (positronic) continuum, as already mentioned.

Appendix A

In this appendix we briefly put forward some materials that can help the reader follow the discussion in Sec. III. For details see [6, 11, 16].

A 1. The axial symmetry around the internuclear axis (the z-axis) in two-center case suggests to use of the well-known prolate spheroidal (elliptic spheroidal) coordinates ξ, η, φ,

$$x = \frac{R}{2}u(\xi,\eta)\cos\varphi,\ y = \frac{R}{2}u(\xi,\eta)\sin\varphi, z = \frac{R}{2}\xi\cdot\eta,$$
$$\text{where } u(\xi,\eta) = \sqrt{(\xi^2-1)(1-\eta^2)}$$

where R is the inter-nuclear distance in atomic units and φ is the electron's angular coordinate. The angular coordinate is separable and the problem is reduced to a 2-dimensional one. The distances of the electron to the nuclei are given by $r_1 = (\xi+\eta)\frac{R}{2}$, $r_2 = (\xi-\eta)\frac{R}{2}$. The Coulomb singularity of point nucleus model causes a singular behavior of the relativistic solutions at the position of the nuclei of the form $r_l^{-1+\gamma_{l,\kappa}}$, with $\gamma_{l,\kappa} = \sqrt{\kappa^2-(\alpha Z_l)^2}$ and $|\kappa| = |j_z|+\frac{1}{2}$, $l = 1, 2$, it is well-known from atomic calculations [12, 44]. Thus, further singular coordinate transformation is needed [6, 11, 16] as the following,

$$Y = 1 + \sum_{i=1}^{\nu/2} d_i\, S^{\nu+2(i-1)}(x/2) \tag{A1}$$
$$\text{for } \nu = 2, 4, 6, 8, 10$$

where Y stands for ξ or η and S for sinh or sin and x for s or t, respectively. With $0 \le s < \infty$, $0 \le t \le \pi$. The transformation can be calculated by integration of the following derivatives,

$$\frac{dY}{dx} = D_n\, S^{2n+1}(x),\ D_n = \frac{(2n+1)!}{n!\, 2^n},\ \text{with } n = \frac{\nu}{2} - 1$$

which determines the coefficients d_i in eq A1. Mathematically they are connecting to the hyper-geometric function $_2F^1$ [6], which can be found by performing the integration using e.g. *Mathematica*. The transformation regularizes the singularities at the nuclei by increasing the point density in the inner region. The higher ν, the denser the points near the nuclei, which ensures a better approximation of (the singularity of) the wave function [16]. An advantage of this transformation is the use of a square grid type over s and t, since $\lim_{s\to 0}(\xi-1) \sim s^\nu$, $\lim_{t\to 0,\pi}(1-\eta) \sim t^\nu$.

A 2. In the present FEM treatment, the 2-dimensional domain (s,t) is subdivided into triangular elements e. The component k of the relativistic wave function is approximated by

$$\phi^k(s,t) = G^k(s,t) \sum_{\text{e}} \sum_{i}^{n} d_i^{k,\text{e}} N_i^{k,\text{e}}(s,t) \ , \tag{A2}$$

where e is the number of the element, n is the total number of the nodal points of the element e and $d_i^{k,\text{e}}$ are the unknown coefficients at the nodal points i. The shape functions $N_i^{\text{e}}(s,t)$ are defined inside the element e by complete polynomials of an order p in s,t and zero elsewhere [10]. The functions $G^k(s,t)$ account for the global behavior of the wave function. They are given by

$$\begin{aligned}
G^k(s,t) &= G_1^k(s,t) \cdot G_2(s,t), \\
G_1^k(s,t) &= \left((\xi^2-1)(1-\eta^2)\right)^{\frac{m_k}{2}}, \\
G_2(s,t) &= r_1^{-1+\gamma_{1,\kappa}} \cdot r_2^{-1+\gamma_{2,\kappa}}, \\
m_k &= j_z + (-1)^k/2 \ .
\end{aligned} \tag{A3}$$

where $G_1^k(s,t)$ represents the angular momentum dependence and $G_2(s,t)$ expresses the singular behavior at the two nuclei, and $\gamma_{l,\kappa}$ as given above. The larger Z, the smaller $\gamma_{l,\kappa}$ and the singular behavior of the wave function is stronger, hence the convergence becomes less efficient.

---

[1] J. Dolbeault, M. J. Esteban, E. Séré, and M. Vanbreugel, Phys. Rev. Lett. **85**, 4020 (2000).
[2] J. Dolbeault and M. Esteban, Int. J. of Quan. Chem. **93**, 149 (2003).
[3] M. Esteban and E. Séré, Commun. Math. Phys. **60**, 499 (1999).
[4] M. Griesmer, R. T. Lewis, and H. Siedentop, Doc. Math. **4**, 275 (1999).
[5] J. D. Talman, Phys. Rev. Lett. **57**, 1091 (1986).
[6] O. Kullie, in *Dissertation (Thesis), Universität Kassel* (http://nbn-resolving.de/urn:nbn:de:hebis:34-1835, 2004).
[7] O. Kullie, D. Kolb, and A. Rutkowski, Chem. Phys. Lett. **383**, 215 (2004).
[8] O. Kullie and S. Schiller, Phys. Rev. A **105**, 052801 (2022).
[9] O. Smits, P. Indelicato, W. Nazarewicz, M. Piibeleht, and P. Schwerdtfeger, Physics Reports **1035**, 1 (2023).
[10] D. Heinemann, in *Dissertation (Thesis), Universität Kassel* (1987).
[11] O. Kullie and D. Kolb, Eur. Phys. J. D **17**, 167 (2001).
[12] L. Yang, D. Heinemann, and D. Kolb, Phys. Rev. A **48**, 2700 (1993).
[13] L.-J. Yang, in *Dissertation (Thesis), Universität Kassel* (1991).
[14] A two-variable, p-order, complete polynomial is defined by:
  $\mathcal{P}(s,t) = a_{00} + a_{10}\,s + a_{01}\,t + a_{11}\,s\,t + a_{20}\,s^2 + a_{02}\,t^2 + \cdots + a_{p0}\,s^p + a_{0p}\,t^p$.
[15] E. Tiesinga, P. J. Mohr, D. B. Newell, and B. N. Taylor, Rev. Mod. Phys. **93**, 025010 (2021).
[16] O. Kullie and D. Kolb, J. Phys. B: At. Mol. Opt. Phys. **36**, 4361 (2003).
[17] O. Kullie, C. Düsterhöft, and D. Kolb., Chem. Phys. Lett. **314**, 307 (1999).
[18] H. Zhang, O. Kullie, and D. Kolb, Journal of Physics B **37**, 905 (2004).
[19] H. D. Nogueira and J.-P. Karr, Phys. Rev. A **107**, 042817 (2023), arXiv.2303.04521.
[20] F. Fillion-Gourdeau, E. Lorin, and A. D. Bandrauk, Phys. Rev. A **85**, 022506 (2012).
[21] D. Mironova, I. Tupitsyn, V. Shabaev, and G. Plunien, Chemical Physics **449**, 10 (2015).
[22] I. Tupitsyn and D. Mironova, Optics and Spectroscopy **117**, 351 (2014).
[23] A. N. Artemyev, A. Surzhykov, P. Indelicato, G. Plunien, and T. Stöhlker, J. Phys. B **43**, 235207 (2010).
[24] A. Ishikawa, H. Nakashima, and H. Nakatsuji, J. Chem. Phys. **128**, 124103 (2008).
[25] F. A. Parpia and A. Mohanty, Chem. Phys. Lett. **238**, 209 (1995).
[26] A. Rutkowski, Chemical Physics Letters **307**, 259 (1999).
[27] I. A. Valuev, Z. Harman, C. H. Keitel, and N. S. Oreshkina, Phys. Rev. A **101**, 062502 (2020).
[28] S. G. Karshenboim, Physics Reports **422**, 1 (2005).
[29] M. Athanasakis-Kaklamanakis and G. Neyens, (2024), arXiv:2402.12157.
[30] S. Alighanbari, G. S. Giri, F. L. Constantin, V. I. Korobov, and S. Schiller, Nature **581**, 152 (2020).
[31] V. I. Korobov, Phys. Rev. A **74**, 052506 (2006).
[32] D. T. Aznabayev, A. K. Bekbaev, and V. I. Korobov, Phys. Rev. A **99**, 012501 (2019).
[33] V. I. Korobov and J.-P. Karr, Phys. Rev. A **104**, 032806 (2021).
[34] A. N. Artemyev, A. Surzhykov, and V. A. Yerokhin, Phys. Rev. A **106**, 012813 (2022).
[35] A. N. Artemyev and A. Surzhykov, Phys. Rev. Lett. **114**, 243004 (2015).
[36] O. Kullie, H. Zhang, and D. Kolb, Chem. Phys. **351**, 106 (2008).
[37] R. A. Hegstrom, Phys. Rev. A **19**, 17 (1979).

[38] J.-P. Karr, Phys. Rev. A **104**, 032822 (2021).

[39] K. Pachucki, Phys. Rev. A **108**, 062806 (2023).

[40] T. Beier, Physics Reports **339**, 79 (2000).

[41] V. I. Korobov, L. Hilico, and J.-P. Karr, Phys. Rev. Lett. **118**, 233001 (2017).

[42] U. D. Jentschura, P. J. Mohr, and G. Soff, Phys. Rev. Lett. **82**, 53 (1999).

[43] U. D. Jentschura, P. J. Mohr, and G. Soff, Phys. Rev. A **63**, 042512 (2001).

[44] C. Düsterhöft, D. H. L. Yang, and D. Kolb, Chem. Phys. Lett. **229**, 667 (1994).